# 4

# The Role of Adaptation in Color Constancy

Qasim Zaidi

To function effectively in the world, people need to reliably identify objects and materials across illumination conditions. The subject areas known as lightness and color constancy deal with the identification of the mean and spectral reflectance of materials, respectively. Although, over time, the spectral and mean reflectance of a material can change, in many cases these physical properties are sufficiently stable to aid in identification. Physical properties of stimuli, however, are not available directly to observation, and need to be inferred from light inputs and neural transformations on these inputs. Even in those cases where reflectance is constant, physical inputs to the eye are altered by illumination conditions that include the mean and spectral radiance of the illuminant, and the source-object-sensor geometry. What are the neural transformations of the physical input that enable identification of like reflectances across different illumination conditions? Is adaptation a crucial neural transformation in this process? Is adaptation based on spatially extended scene statistics or on local information collated over time? These are the kinds of questions addressed in this chapter.

## 4.1 Adaptation and Lightness Identification for Real 3-D Objects under Natural Viewing Conditions

When viewing achromatic surfaces it is possible, in some instances, to separate the *lightness* of a surface from its *brightness*. Lightness is the mean reflectance,

where reflectance is the fraction of incident light reflected back by the surface, and is solely a property of the surface (Evans 1974). Brightness refers to apparent luminance, where luminance is the light reflected from the surface, and is thus a function of both the incident illumination and the surface reflectance. Perceived brightness differs from the physical quality of luminance because brightness is affected by adaptation (Craik 1938; Helson 1964) and by lateral interactions (Chevreul 1839; Zaidi 1999). Reflectance is also a physical quality, and the lightness of a surface is inferred either visually or cognitively by separating the information on the scene into environmental and material changes (Helmholtz 1962; Hering 1964).

Consider the demonstration in Fig. 4.1. Look at the four crumpled objects in the two compartments. Three of the objects are made of identical gray paper while one is made of a different shade of gray paper. The compartment on the right is receiving half the illumination of the compartment on the left. Which is the odd object? In order to correctly perform this task, you can first use brightness discrimination to select the compartment that contains the pair of objects with reflectances different from each other. However, once this compartment has been chosen, you have to identify the lightness within that compartment that is different from the two objects in the other compartment.

In Fig. 4.2, the two objects from the right compartment in Fig. 4.1 have been kept in the same place, while the two objects from the left compartment have been placed behind them to facilitate comparison under a single illuminant. It is clear from Fig. 4.2 that object 3 was the odd object, lighter than the other three. If you did not identify the object correctly, your response shows a failure of lightness constancy.

1 2 3 4

FIG. 4.1 Three of the crumbled objects are made of identical grey paper and make up a *standard* set, while one *test* object is made of a different grey paper. Backgrounds in the two compartments have the same reflectance distribution. The compartment on the right is receiving half the illumination of the compartment on the left. Which is the test object?

3 1 2 4

FIG. 4.2 For demonstration purposes, objects 1 and 2 from the left compartment of Fig. 4.1 have been placed behind objects 3 and 4 in the right compartment. When all four objects are under the same illumination, it becomes obvious that object 3 is the test object with a higher reflectance than the three identical standard objects.

Robilotto & Zaidi (2004) performed the experiment shown in Fig. 4.1 by using real objects and lights, viewed binocularly with no constraints on eye-movements. We used a method of constant stimuli and varied the lightness of the test for each standard lightness. When the proportions of correct responses are plotted against the reflectance difference between Standard and Test, the proportions of correct "side" responses gives brightness discrimination psychometric functions, while the proportions of correct "object" responses give lightness identification psychometric functions. In order for the two functions to be scaled on the same ordinate, detection and identification rates can be normalized for guessing. Normalized response data for two hypothetical observers are shown in Figs. 4.3(A) and (B). Dashed curves represent the proportions of side-correct responses, and solid curves represent proportions of object-correct responses. The top plot represents conditions where the Test object is under the brighter illuminant, and the bottom represents conditions where the Test object is under the darker illuminant.

What information is available in the display, and what is the best identification performance that any visual system could achieve? Backgrounds in the two boxes were made from the same materials, so they have similar statistics. The hypothetical observer represented by the curves in Fig. 4.3(A) calculates the mean luminance of both backgrounds and the mean luminance of each of the four cups, calculates the ratio of the luminances of the backgrounds, uses this as an estimate of the ratio of the radiances of the illuminants, and applies the ratio to the luminances of the objects to equate the reflectances of the three Standard objects, and thus identifies the odd object. Because there is sufficient information in the scene for this strategy of lightness identification, this observer's lightness identification performance is limited only by the ability to discriminate within

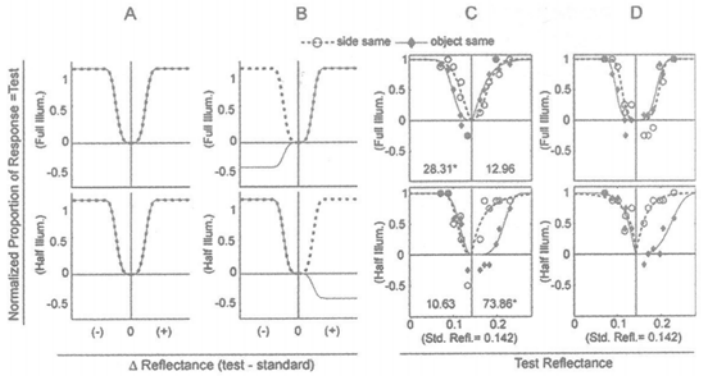


FIG. 4.3 Hypothetical observers and real data. Proportions of correct responses (corrected for guessing) are plotted versus the reflectance of the test. Dashed lines and open circles represent proportion of correct side responses (Brightness discrimination), while solid lines and filled diamonds represent proportion of correct object responses (Lightness identification). The top row represents conditions in which the test object is in the compartment under full illumination, while the bottom row represents conditions in which the test object is in the compartment under half illumination. The vertical line in each plot indicates the reflectance level of the standard set. (A) Responses of a hypothetical observer with perfect lightness identification limited only by discrimination. (B) Responses of a hypothetical observer based on picking the object most dissimilar in luminance. (C) Typical Lightness identification results. Psychometric curves were fit to both sets of data using maximum likelihood ratios. Under the hypothesis that identification responses across illuminants are limited only by the ability to discriminate among objects within the same illuminant, the incorrect object identification responses should be randomly distributed among the three Standard objects. The chi-squared values in each panel test this hypothesis with an asterisk denoting rejection of the hypothesis. (D) Typical normalized proportions of responses where the object chosen as most different in brightness was the object of odd reflectance.

illuminants, and the response functions for brightness discrimination and lightness identification are superimposed. If, however, an observer acted like a photometer, measured just the mean luminances of the four objects, and simply chose the object most different in luminance as the odd object, results would look like in Fig. 4.3(B). When a Test is under full illumination (top plot) and has a lower reflectance than the Standard, its luminance will be lower than the Standard in its compartment and closer to the luminance of the two Standards in the other compartment. When a Test is under half illumination (bottom plot) and has a higher reflectance than the Standard, its luminance will be higher than the Standard in its compartment and closer to the luminance of the two Standards in the other compartment. Under these types of conditions, for some values of Test reflectance at which brightness discrimination reliably identifies the correct side, the Standard on that side will be chosen as the odd object consistently and incorrectly. In Fig. 4.3(B), this is indicated by the curves below chance level, i.e. below zero normalized proportion correct.

Fig. 4.3(C) presents typical data from an observer. There seems to be an asymmetry in the data, as lightness identification seems to be systematically worse than brightness discrimination for lower reflectance Tests under full illumination and higher reflectance Tests under half illumination. Using a chi-squared test, the hypothesis that identification responses across illuminants are limited only by the ability to discriminate among objects within the same illuminant was rejected 10 out of 12 times for conditions where either Tests under full illumination were of lower reflectance than the Standards or where Tests under half illumination were of higher reflectance than the Standards, but only 1 out of 12 times for the other two conditions. The question thus arises whether a single perceptual strategy can account for failures and successes in lightness identification.

In the second experiment, we investigated whether observers were using a lightness-based strategy, or a brightness-based strategy. All stimuli and conditions remained the same, but instead of instructing the observers to choose the object with a different material, observers were asked to choose the object with a different brightness. Figure 4.3(D) shows the proportion of trials on which the Test object was chosen as most dissimilar in brightness. These curves are similar to the lightness identification curves, particularly in their asymmetry. Figure 4.4 plots the odd-brightness thresholds against the odd-lightness thresholds, and shows that reflectance values were similar for both observers. It is likely, therefore, that observers were using brightness dissimilarity to do the lightness identification task.

The lightness identification curves of the photometer-like observer discussed earlier do not resemble the measured curves except for similar directions of asymmetries. It is well-known that light adaptation affects brightness discrimination and appearance (Craik 1938; Helson 1964). Therefore, we tested

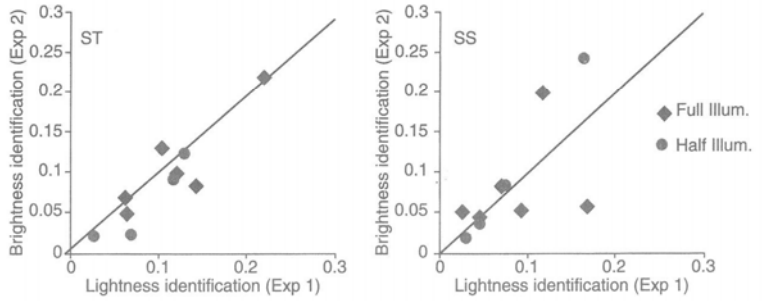


FIG. 4.4 Reflectance threshold values for correct lightness identification, based on lightness versus brightness dissimilarity.

whether a photometer-like observer could give results similar to our observers if we incorporated a mechanism of adaptation which computes the brightness of a stimulus as the product of its mean luminance and a scalar gain, where the gain is a monotonically decreasing function of mean luminance within a compartment (Hayhoe *et al.* 1987). The gain, $G$, for illumination, $I$, is governed by the free-parameter, $\kappa$, i.e. $G = \kappa/(\kappa + I)$.

Figure 4.5 illustrates hypothetical brightness dissimilarity responses based on this model for three different values of $\kappa$. If there were no adaptation ($\kappa = \infty$), judgments would be based solely on luminance values of the objects. As $\kappa$ decreases, adaptation increases and less reflectance difference is needed for the object most different in reflectance to become the object most different in brightness. The model's brightness dissimilarity responses now start to approximate the reflectance identification responses of the observers, in particular the asymmetry in the curves with respect to the brightness discrimination curves, and the dip of a few points below chance.

Under everyday conditions, observers consistently judge surfaces as having a certain lightness or grayness. This subjective impression points out the tendency to use the physical property of reflectance in mental representations of surfaces. This phenomenological experience however is not sufficient evidence that the visual system has access to the reflectance or lightness of materials. For our 3-D objects, there are some conditions where lightness identification is limited solely by the limen of brightness discrimination, but in other conditions

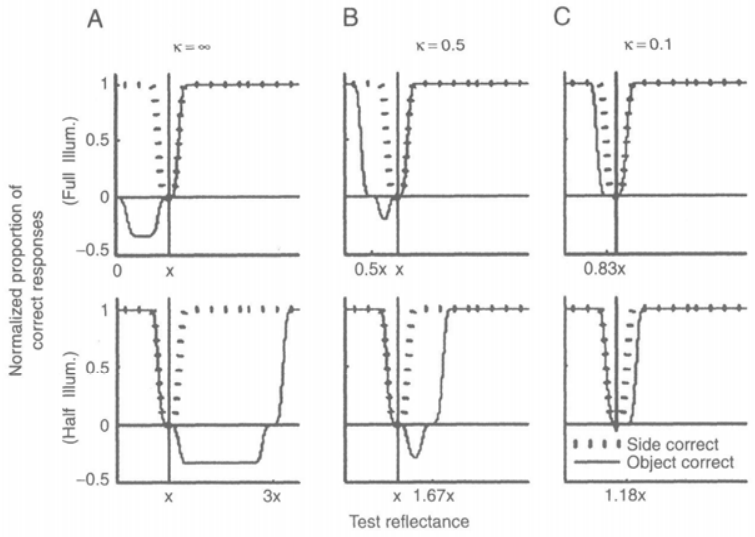


FIG. 4.5 Normalized proportion of correct responses, based on a model of brightness dissimilarity incorporating multiplicative adaptation. (*Left*), (*center*), and (*right*) represent models based on three levels of gain with decreasing $k$ values. Standard reflectances are denoted by $x$.

lightness identification is considerably worse. We have shown that the same relative brightness based strategy reproduces both sets of results. This conclusion is based on the fact that the psychometric curves for lightness identification and brightness dissimilarity are systematically asymmetric relative to brightness discrimination curves measured simultaneously for the same objects, and this asymmetry can be predicted quantitatively from observers' choices of most dissimilar brightnesses, and qualitatively from the choices of a photometer-like model observer incorporating brightness adaptation. Note that reflectance dissimilarities are not asymmetric around the standard reflectance, so lightness percepts could not be the basis of the asymmetric brightness dissimilarity judgments in Fig. 4.3(D). The visual system may have evolved to identify object properties, but this identification can only be based on sensory information and transformations, and adaptation is a critical aid in correct identification.

## 4.2 Differences between Brightness and Color Information for Material Identification

In the generic case, illuminants differ not only in radiance, but also in spectral composition. When the spectrum of the illuminant changes, so do the spectra of lights reflected from surfaces. Just as the brightness of a surface is a function of the luminance of the light reflected from the surface, adaptation and surround effects; the perceived color of a surface is a function of the spectrum of the light reflected from the surface, adaptation and surround effects. The term color constancy describes the extent to which object colors appear unchanging despite changes in the spectral composition of the illumination (Helson *et al.* 1952; Land & Mc Cann 1971; Land 1983; Kraft & Brainard 1999; Foster 2003). There exist good reasons to expect color to be better than brightness as a cue for material identification across illuminants. Zaidi (1998) showed an example where in a grey-level picture, bright leaves appear like they are under a brighter patch of light, whereas, in the color image, the leaves are revealed to have a light-yellow reflectance that is under the same illuminant as the surrounding area. The use of color information can thus supplement other strategies (Sinha & Adelson 1993) for separating reflectance changes from illuminant changes. More formally, Kingdom (2003) has shown that chromatic variations are used by the visual system to differentiate luminance variations that are due to shadows and shading from those that are due to surface reflectance. In addition, Sachtler and Zaidi (1992) showed that memory for chromatic qualities is superior to memory for gray levels: for short time intervals, memory thresholds for hue and saturation are almost as fine as discrimination thresholds, whereas memory for gray levels is considerably worse than discrimination. This raises the possibility that in the functionally important task of identifying similar objects dispersed across space and/or time, the color attributed to the objects may be vital. The appearance of a material can also be altered by color induction from the surround. In the case of brightness, the total induced effect is the weighted sum of

surrounding effects, with areas closer to the material having greater weight. On the other hand, the total induced effect on the perceived color of a material is not the weighted sum of surrounding effects, and in fact is reduced drastically if there are high spatial-frequency chromatic variations in the surround (Zaidi *et al.* 1992).

### 4.3 Material Color Conversions due to Changes in Illuminant Spectra

In a situation where a spatially uniform light falls on flat surfaces of Lambertian reflectance (i.e. reflect light equally in all directions), the spectrum of the light incident on an observer's eye is the wavelength-by-wavelength multiplication of the illuminant spectrum and the surface reflectance spectrum at each point in the scene. In the human retina, the incident spectrum is absorbed by three types of cone photoreceptors, called *L*, *M*, and *S* for cones that are most sensitive to the Long, Middle, and Short wavelengths of the visible spectrum (Baylor *et al.* 1987). The outputs of the cones are combined by post-receptoral neurons into two classes of color signals (*L* versus *M*, and *S* versus *L*+*M*) and a luminance signal (*L*+*M*) (Derrington *et al.* 1984). These signals are transmitted to the cortex, where they are combined in a myriad of ways to subserve the many functions of the visual system.

Since the spectrum reflected from each surface is a multiplication of the illuminant and reflectance spectra, the effect of a change in illumination spectrum is different for each surface reflectance. The situation turns out to be simpler if, instead of changes in the spectra of light, one considers changes in the cone-coordinates. For sets of everyday objects, and natural and man-made illuminants, when the *L*- (or *M*-, or *S*-) cone-coordinate (Smith and Pokorny 1975) for each object under one illuminant is plotted against the *L*- (or *M*-, or *S*-) cone coordinate for that object under a different light, the points all fall close to a straight line through the origin (Dannemiller 1993; Foster & Nascimento 1994; Zaidi *et al.* 1997). The top row of Fig. 4.6 shows the *L*, *M*, & *S* cone absorptions calculated from the reflectance spectra of a sample of 280 natural and man-made materials (Chittka *et al.* 1994; Vrhel *et al.* 1994; Hiltunen 1996; Marshall 2000) under Zenith Skylight plotted against the values under Direct Sunlight (Taylor & Kerr 1941). Within each cone class, a change in the spectrum of the illuminant leaves signals from different objects unchanged in their relative positions with just local exceptions, i.e. the effect is to multiply all object cone-coordinates by the same constant. This systematic shift is most likely due to integration within fairly broad cone absorption spectra, because it exists even for spiky illuminant spectra, like fluorescent lights (Zaidi 2001). Nascimento *et al.* (2002) showed that these multiplicative shifts also hold for illuminant changes on natural scenes. The Macleod–Boynton (1979) chromaticity axes ($L/(L+M)$, $S/(L+M)$) provide a good representation of the post-receptoral color signals (*L* versus *M*, and *S* versus *L*+*M*). Zaidi *et al.* (1997) showed that when the effects of changes in illuminant spectrum are transformed to Macleod–Boynton coordinates, the $L/(L+M)$ chromaticities are shifted by an additive constant, whereas the

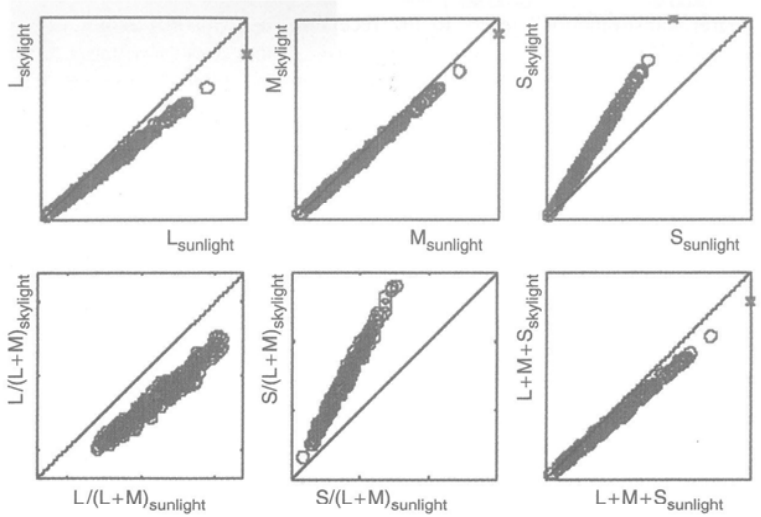


FIG. 4.6 Top row plots show excitations of L-, M-, and S-cones from each of 280 reflectance spectra rendered under two illuminants: zenith skylight on the ordinate and direct sunlight on the abscissa. Bottom row plots show excitations of post-receptoral chromatic and luminance mechanisms ($L/(L+M)$, $S/(L+M)$, and $L+M+S$) from the same stimuli. In each plot, the X represents the illuminant.

$S/(L+M)$ chromaticities are shifted by a multiplicative constant (bottom row of Fig. 4.6). The additive shift in $L/L+M$ is due to the extremely high correlation between *L* and *M* cone-coordinates for sets of surfaces under each illuminant (Zaidi 2001).

The situation above assumes that the color of each object is well-represented by a single triple of cone-coordinates. This assumption is valid for flat Lambertian surfaces of unvarying spectral reflectance lit by a uniform illuminant. However, most materials in the world have some surface texture and are not Lambertian, and most objects are not flat. Though good physics-based models for reflections from textured surfaces are extremely complex (Koenderink & van Doorn 1996), a decent approximation can be made by the assumption that for each facet, the total reflection is a weighted sum of the body reflection and the interface reflection (Oren & Nayar 1995), i.e. a weighted sum of the surface and illuminant cone-coordinates. Under this assumption, the affine transforms caused by illuminant changes for Lambertian surfaces also hold for rough surfaces if the source-object-sensor geometry is constant, e.g. if there is a change in the spectrum of the illuminant falling on a stationary scene, and the observer's viewpoint is unchanged (Zaidi 2001).

We will use the term "color conversion" (Helson 1938) to refer to changes in the spectra of the lights reflected from surfaces as the spectrum of the illuminant changes, and to subsequent changes at level of cone-absorptions. The term

"neural transformation" refers to the receptoral and post-receptoral neural processes that serve to transform the perceived colors of objects under a test illuminant towards the colors of objects under a reference illuminant. The highly systematic nature of the color conversions described in Fig. 4.6, indicates that simple neural transformations could support color constancy, and the types of neural mechanisms that could, in principle, perform such transformations, range from automatic to volitional, and from peripheral to central.

In 1878, von Kries suggested that the invariance of color metamers to mean light level might be due to multiplicative gain control at the photoreceptor level, when these gains are set independently within each class of photoreceptor in inverse proportion to the local stimulation (von Kries 1878, 1905), i.e. a mechanism incorporating adaptation that computes the output of a cone as the product of its instantaneous input and a scalar gain, where the gain is a monotonically decreasing function of the mean input over time. Ives (1912) may have been the first to suggest an explicit mechanism for constancy under an illuminant change. He showed that the multiplicative factors that transform the *illuminant's* cone-coordinates to those of an equal energy illuminant also transform the cone-coordinates of *surfaces* to approximately their cone-coordinates under the equal-energy illuminant. Figure 4.6 helps to illustrate why this simple transform will work. The illuminants are plotted at the extreme end of the line of reflectances as crosses. Multiplying each cone-coordinate by the ratio of the illuminant cone coordinates will transform most surface cone-coordinates to the unit diagonal, thus equating neural signals under the two illuminants. Mathematically, the Ives transform consists of multiplying all cone-coordinates by the same diagonal matrix and has been widely analyzed in the computer vision literature where it is misnamed the von Kries transform. von Kries' original transform multiplies each local cone-coordinate by a scalar depending only on its *local* magnitude, and thus shifts all colors towards a neutral color (Vimal *et al.* 1987; Webster 1996) rather than achieving the required transformation to an equal energy illuminant.

## 4.3 Estimation of Illuminant Color

The Ives transformation relies on the visual system's ability to estimate the cone-coordinates of the illuminant. Since the illuminant itself is often not in the field of view, its cone-coordinates have to be estimated from scene statistics. Khang and Zaidi (2004) examined how observers extract the color of spectrally filtered spotlights that are cast on different variegated sets of materials. In an asymmetric spotlight matching technique, observers were asked to adjust the color of a Match spotlight moving over materials with uniform reflectance spectra, to match the color of a Standard spotlight moving on spectrally selective materials (Fig. 4.7, top left). Because the illuminated materials are different under the two spotlights, this match cannot be accomplished by point-by-point color matching, but instead requires matching the extracted colors of the illuminants. The only objects visible were those that fell under the spotlights. The spectra of the seven spotlights were obtained by double-passing equal energy light through

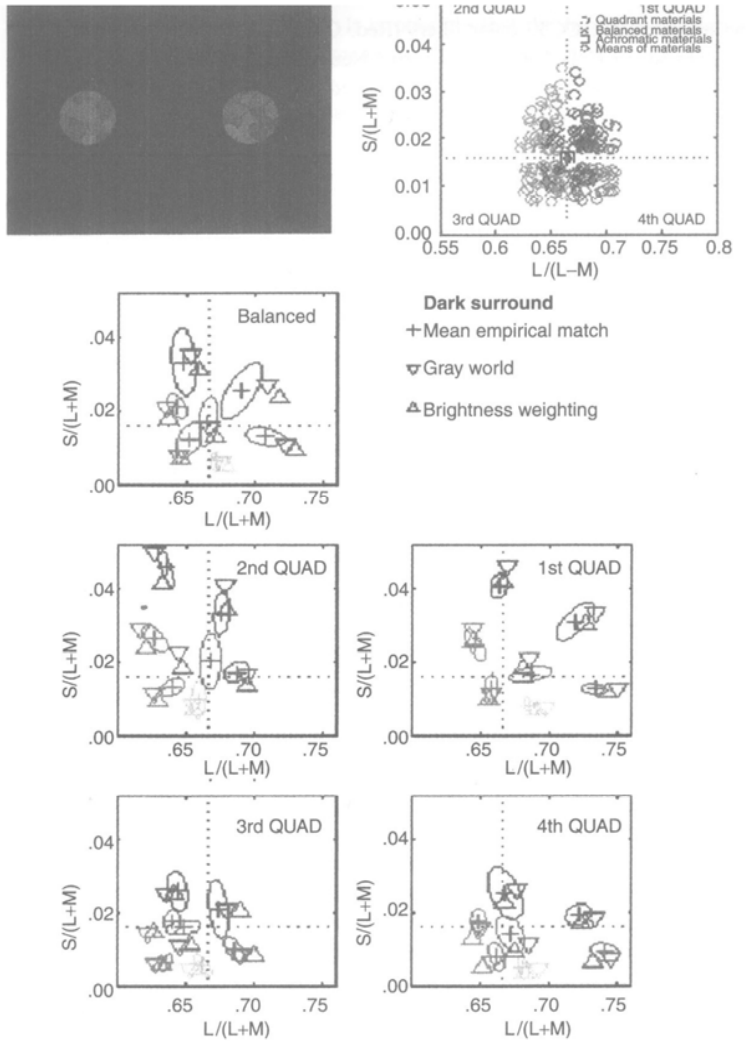


FIG. 4.7 (Top left) Red spotlight cast on green-yellow materials on the left and the same red spotlight on gray materials on the right. Observers were asked to estimate the color of the spotlight moving on chromatic materials and to match it by adjusting the color of the spotlight moving on gray materials. (Top right) MacLeod–Boynton chromaticities (under equal energy light) of the 240 materials used, which consisted of 6 sets of 40 materials. 4 sets of chromatic materials from each quadrant, one set of balanced chromatic materials, one set of achromatic materials. Colored diamonds indicate mean of each quadrant's materials, while the square and the gray diamond at the intersection of the horizontal and vertical dotted lines represent both the achromatic materials and the mean of the balanced chromatic materials. (Bottom) Mean chromaticities of the match spotlights (+), and predictions from a gray-world model (△) and a model that gives greater weight to the brighter materials (▽). The results are color-coded to correspond roughly to the appearance of the spotlight on the achromatic materials. (See also Plate 1 at the centre of this book.)

one of six Kodak CC30 color filters (Red, Green, Blue, Yellow, Magenta, and Cyan) (Kodak CC30, 1962) or through a Neutral Density filter with 70 per cent transmittance. The Standard spotlight moved over one of four sets of 40 materials from single quadrants of MacLeod–Boynton color space, or a fifth set equally balanced across quadrants (Fig. 4.7, top right), chosen from 4824 reflectance functions of flowers, leaves, fruits (Chittka *et al.* 1994), natural and man made objects (Vrhel *et al.* 1994), Munsell color chips (Hiltunen 1996), and animal skins (Marshall 2000). Match spotlights moved over 40 achromatic materials with reflectances equated to the balanced chromatic set. The simulation gave a vivid impression of spotlights moving over matte flat colored and achromatic surfaces in a dark scene. This experiment can reveal estimation strategies for illuminant color when only one illuminant is in the field of view, and there are no clues provided by highlights, shading and shadows. Since the patterns of results were similar for all three observers, we combined the results and calculated means and ±1 SD ellipses over all observers, and these are shown separately for each chromatic set in MacLeod–Boynton diagrams in Fig. 4.7 (bottom). For the chromatically balanced background, the ±1 SD ellipses included the veridical match. For the biased backgrounds, very few of the ellipses for the empirical matches contained the corresponding veridical matches. The mean empirical matches deviated from the veridical systematically in the direction suggesting a biasing effect of background chromaticities on illuminant estimation.

The simplest model for illuminant color estimation is the gray-world model, where estimates of the illuminant cone-coordinates are obtained by taking the means of all the cone-coordinates under the illuminant (Buchsbaum 1980). The veridicality of this estimate relies on the assumption that the mean surface reflectance is likely to be uniform. In Fig. 4.7, the predicted points from the gray-world hypothesis are close to the data points, and this model provides a reasonable, but not perfect, explanation for illuminant color estimation. The gray-world assumption is unlikely to be true for most natural scenes (Brown 1994; Webster & Mollon 1997; Webster 2002), so Golz & MacLeod (2002) have suggested that luminance-chromaticity correlations, e.g. luminance versus redness, may provide estimates that are less influenced by the set of reflectances available. Models for illuminant estimation, however, should incorporate the fact that high-intensity regions of scenes potentially contain more illuminant color information than do low-intensity regions. Tominaga *et al.* (2001) present the following thought experiment: The image of a black surface will have close to zero sensor responses under any illuminant, and its chromaticity will be a function of random noise; whereas a white surface will map reliably to the chromaticity corresponding to the illuminant spectrum. Hence, combining the two measurements will produce a worse estimate than using the bright region alone. In a simulation study of black-body illuminants, Tominaga *et al.* demonstrated that sensor responses from the brightest intensity regions were most diagnostic in classifying illuminants of different color temperature. We implemented these ideas by generalizing the gray-world model to incorporate weighting by the luminance of each material with the luminance raised to a positive power. The brightness-weighted model in Fig. 4.7 fits the data at least as well as the gray-world model. It is possible that the brightness-weighted model would give a better fit for scenes that contain specular highlights (Lee 1986; Lehman & Palm 2001).

A neural mechanism that integrated over a large spatial area could in principle extract the mean chromaticity. If the outputs of local subunits of such a mechanism were subjected to accelerating nonlinearities before integration, then this mechanism would estimate the illuminant by weighting scene chromaticities as an increasing function of their brightness. The question remains whether such estimates are incorporated by adaptation mechanisms to discount the effect of illuminant changes, since psychophysical measurements indicate that early adaptation mechanisms are extremely local in their spatial properties (MacLeod *et al.* 1992; MacLeod & He 1993; He & MacLeod 1998).

## 4.4 Role of Global Adaptation to Scene Statistics

Adaptation can account for color constancy if chromatic signals from objects vary by less than a discriminable difference across two illuminants. For the case of a fixed scene and a slowly varying illuminant, Zaidi *et al.* (1997) tested whether adaptation to a variegated scene was sufficient to counter the effect of changes in illuminant spectra. We asked our observers to view a simulated scene, and report if the colors in the scene appeared to change when the effect of an illuminant change was simulated. As shown in Fig. 4.6, the effect of a change in the phase of natural daylight on post-receptoral mechanisms can be simulated by adding a constant to all $L/(L + M)$ chromaticities, and by multiplying all $S/(L + M)$ and $L + M + S$ chromaticities by constants. This enabled us to quantify the tolerance within each post-receptoral mechanism for changes in illumination. Nascimento and Foster (1997) have shown that large-field color changes that keep spatial ratios of cone excitations perfectly constant are perceived as illuminant changes, and are in fact chosen as illuminant changes even over real illuminant changes. Since we were interested in the effect of spatially complex scenes on color constancy, we used random binary and quaternary distributions of squares of uniform size. The binary textures were colored by extremes of each of the $L/(L + M)$, $S/(L + M)$, and $L + M + S$ axes (termed *RG*, *YV*, and *LD* for mnemonic purposes) and the quaternary textures by sums of pairs of binary texture colors (*LDRG*, *RGYV*, and *YVLD*). The space-averaged chromaticity and luminance of all textures was equal to equal-energy white, *W*. The observer adapted to the background for 2 minutes at the initiation of each session and readapted for 2 seconds after each trial (Fig. 4.8). The illuminant on a scene was changed gradually toward and back from a different illuminant as a half-cycle of a sinusoid over a 3 seconds interval. To control for criterion effects, each trial also included another interval in which the illuminant was not altered. The observers indicated the interval in which they perceived a change in the colors of the scene. Thresholds measured for illumination changes in the *R*, *G*, *Y*, *V*, *L*, and *D* color directions on each textured field were compared with thresholds on a uniform achromatic field at *W*.

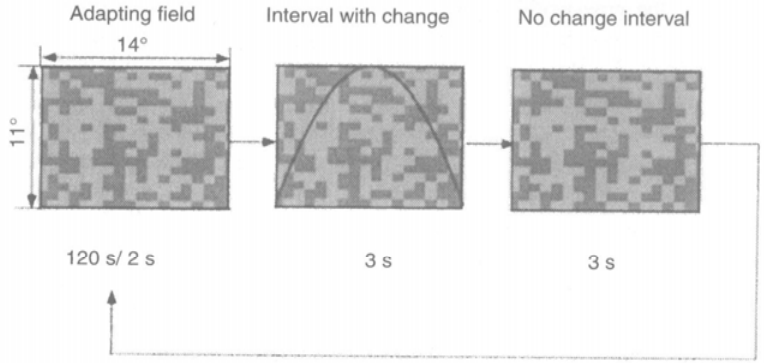


FIG. 4.8 Spatial configuration and temporal sequence of stimuli for global adaptation experiments. The initial adaptation period was 120 s. Each trial consisted of a 2-s period of readaptation, followed by two 3-s intervals, of which one contained a simulated illumination change with a time-course of a half-sinusoid.

Results for two observers are shown in Fig. 4.9. The colors of the background textures are indicated on the abscissa. For each texture class, the threshold for detecting a change in colors as compared with the threshold for detecting a change on the achromatic field is plotted on the ordinate. Separate panels show data for the *L*, *D*; *R*, *G*; and *Y*, *V* directions of simulated illuminant changes. We are interested not in whether there is a small but statistically significant increase in thresholds on the background but whether certain backgrounds functionally mask the effect of illumination changes: the dashed horizontal line at 0.3 identifies the textures that increased the tolerance for an illumination change by at least a factor of 2. The results are systematic and similar for the two observers. Full-field color changes (*R*, *G*, *Y*, *V*) are less likely to be perceived in the presence of chromatic spatial variations, but thresholds for detection of full-field luminance changes (*L*, *D*) are not affected by the presence of spatial variations. Except for one case out of 36, changes toward a chromatic direction are affected only when there is spatial contrast along the same axis. There was no systematic effect of superimposing spatial contrast along a color axis orthogonal to the color direction of the simulated illumination change. The results indicate that the masking effect of spatial contrast is relatively independent within each of the opponent-color mechanisms.

The results show that if the scene contains spatial variations, an observer is less likely to perceive changes in the colors of the scene when the illumination changes than if the scene was spatially uniform at the space-averaged color. The effects of a shift from Sunlight to Skylight on natural scenes can be compared with the experimentally measured thresholds, and shown to be extremely salient. The average shift of signals along the $L/(L+M)$ axis in Fig. 4.6 is 21.3 times the threshold for a similar shift on the *W* background for observer BS, and 6.4 times for observer KW. Even for the most desensitizing textured background, only 15 per cent of this shift could be tolerated by observer BS, and

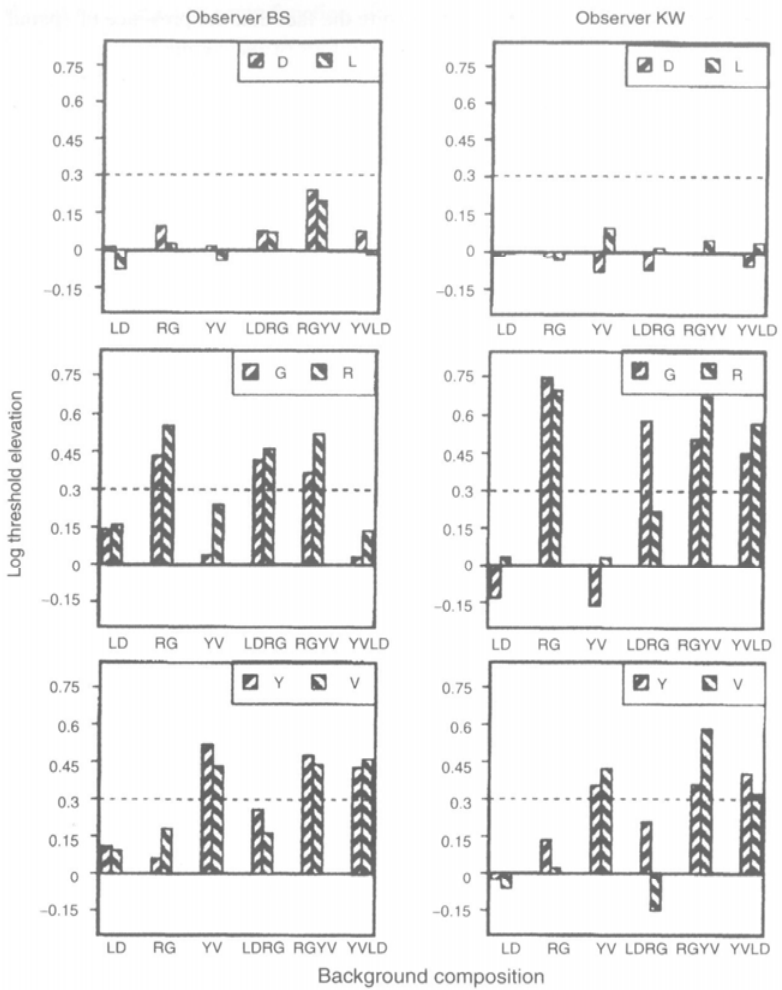


FIG. 4.9 Results for observers BS (left-hand plots) and KW (right-hand plots). The log of the threshold for detecting a change in each color direction minus the log of the baseline threshold for that color direction is plotted against the chromatic content of the background texture (see text). Symbols representing the color direction of the simulated illuminant change are shown in the insets. Dashed horizontal lines are drawn at 0.3 to indicate a doubling of threshold magnitude.

97 per cent by observer KW. The average multiplicative shift along the $S/(L+M)$ axis is 18 times the threshold for a similar shift on the *W* background for observer BS and nine times for observer KW. On the most desensitizing textured background, BS could tolerate only 19 per cent of the shift, and KW 36 per cent. In general, then, an acute human observer will perceive changes in colors of objects when the illumination shifts over a few seconds between

different phases of natural daylight, despite the fact that the presence of spatial variation will attenuate the perceived magnitudes of the changes.

Objects in the world are almost always seen against variegated backgrounds, but almost all studies of color adaptation have used uniform backgrounds. Using stimuli similar to Fig. 4.8, Zaidi *et al.* (1998) showed that adaptation to a variegated field consists of more than adaptation to the space average, or independently to the constituents, or to any combination thereof. We found that a model for the effects of adapting to variegated fields not only has to take into account different sorts of adaptation at different stages of the visual system, but must also incorporate spatial inhomogeneities in adaptation state across the field and a decision process that involves pooling spatially distributed responses. The model included two classes of spatial locations of neurons. Neurons of one class were constantly exposed to uniformly colored patches in the field, and neurons of the second class were near the edges of color patches. Of those exposed to one color, $S$ versus $L+M$ neurons adapted by multiplicative gain controls determined by the time-integrated level of stimulation, whereas $L$ versus $M$ neurons adapted by a subtraction of a portion of the time-integrated signal (Zaidi *et al.* 1992; Shapiro *et al.* 2001, 2003). On the other hand, neurons that were located near the edges of color patches adapted to temporal modulation of their inputs as a result of eye movements, and this resulted in changes in the shapes of their response functions rather than adaptation to the average stimulation (Zaidi & Shapiro 1993). Global adaptation to a variegated field thus is not determined by the spatial averages that observers use for estimating illuminant color, and has quite different functional benefits as described below.

Adaptation at early stages of the visual system serves to enable good discrimination across a very large domain of lights despite the limited response range of individual neurons. Craik (1938) introduced notions of efficiency into range-resetting, and since then it has been thought to be optimal that when adapted to a certain level, an observer's discrimination should be best at that level. However, this property would be functionally optimal only if it could be assumed that the frequency distribution of stimulation in the near future would have a maximum at or near the adapting level. The situation is quite different when an observer is viewing a spatially variegated field. It has been proposed that, as a result of eye movements, the observer should adapt to the space average (D'Zmura & Lennie 1986; Fairchild & Lennie 1992). However, adapting to the average stimulation alone would not be optimal, because it is unlikely that the highest frequency of future stimuli will occur near the average level. In fact, adaptation to any single level is likely to be grossly suboptimal, and it would be more efficient to adapt the range of sensitivity to the domain of expected stimulation. Zaidi and Shapiro (1993) proposed a model of "response equalization" to account for changes in the response function. This model postulates that the most efficient use of a limited response range is to match the shape of the response function to the expected distribution of inputs, so that on an average, each level of response occurs with equal frequency. If it is assumed that expectations for inputs are set by the recent adaptation history, then the response function should be equated to some function of the cumulative probability distribution of levels in the adapting stimulus. Adaptation to a variegated scene thus is more complex than being a function of the mean level or any other estimate of the illuminant. It is thus not a mechanism that can serve to correct for changes in the illuminant spectrum. On the other hand as the next section shows, range-resetting as a function of the time-integrated signal has specific effects on perceived colors.

## 4.5 Roles of Local Adaptation and Levels of Reference

The results above show that adaptation to global scene statistics is limited in its effectiveness as a color constancy mechanism. A very large number of studies have shown fairly decent color constancy for single patches of constant reflectance. In a series of experiments Smithson and Zaidi (2004) performed critical tests of whether neural transformations for color constancy of such patches depend on information that is distributed over space, or on information that is spatially localized but distributed over time. In addition, we investigated whether judgments of color appearance under different conditions are well predicted by early adaptation, or whether they reflect higher-level perceptual mechanisms?

In this study we assessed changes in color *appearance* under different illuminants. Our stimulus displays consisted of a square test patch presented on a variegated background of randomly oriented elliptical patches. Examples of these displays are given in Fig. 4.10 (left). Each patch was assigned a reflectance spectrum and rendered under a particular illuminant. We tested a total of 280 simulated materials (Fig. 4.6). Reflectance spectra were chosen from measurements of natural and man-made objects so as to obtain an even coverage of color space. Our background patterns were colored with subsets of 40 reflectance spectra, chosen as described below. Test materials and backgrounds were rendered under either the spectrum of direct sunlight or of zenith skylight. The observer's task was to classify the appearance of sequentially presented test-patches as either red or green in one set of trials, and as either yellow or blue in a second set (Chichilnisky & Wandell 1999). We thus obtained a chromatic locus of test-patches that appeared neither red nor green, and a second locus that appeared neither yellow nor blue. We assume that color boundaries measured under different conditions describe a set of stimuli that generate equivalent signals at the decision stage, hence shifts in the locations of color boundaries provide a measure of the neural transformations performed under different conditions of observing.

In the first experiment, we obtained classification boundaries for conditions in which scenes were rendered under either direct sunlight or zenith skylight. Repeated classifications for each material provided psychometric functions relating stimulus chromaticity to classification-probability i.e. the percentage of times the stimulus is classified as red (versus green), or yellow (versus blue).

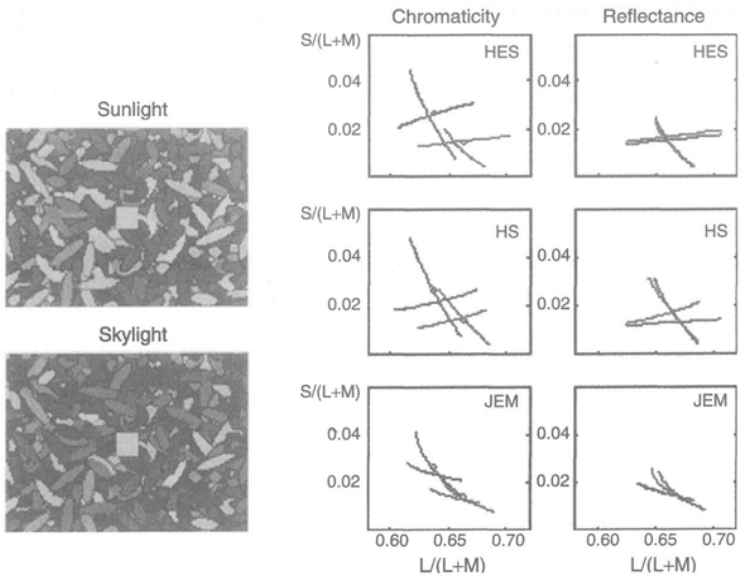


FIG. 4.10 (Left) Examples of stimuli used in color appearance measurements with a global illuminant change on chromatically balanced backgrounds. On each trial, a square test patch was presented on a variegated background of randomly oriented elliptical patches, under skylight or sunlight. (Center) Data for three observers. Panels show traces of classification boundaries in chromaticity space. Red lines show boundaries obtained under sunlight; blue lines show boundaries obtained under skylight. Red and blue open-circles show the corresponding illuminant chromaticities. (Right) Panels show the same boundaries represented in reflectance space (i.e. as if materials were rendered under an equal energy illuminant). (See also Plate 2 at the centre of this book.)

Multiple linear least squares regression was then used to determine the best fitting 3-dimensional polynomial (second- or third-order) relating chromaticity and classification-probability. We assume that the surface in 3-D color space defined by a classification-probability of 0.5 best divides color space into red versus green (or yellow versus blue) and thus represents the classification boundary. The panels of Fig. 4.10 (center) show the lines of intersection of these surfaces with the mean equiluminant plane of the MacLeod–Boynton chromaticity diagram. Traces of classification boundaries are plotted for three observers. Red lines represent boundaries obtained under sunlight illumination; blue lines represent boundaries obtained under skylight illumination. The locations of red/green and yellow/blue boundaries in chromaticity space shift appreciably across illuminants. Panels of Fig. 4.10 (right) show classification boundaries evaluated in reflectance space (i.e. material chromaticities plotted as if rendered under a spectrally uniform illuminant). Classification boundaries obtained under the two illuminant conditions make similar divisions of reflectance space i.e. the grouping of test-materials into color categories is largely unaffected by the illuminant under which they are rendered. This method of demonstrating appearance-based color constancy overcomes many of the shortcomings of conventional methods described by Foster (2003).

A quantitative method to assess the extent of color constancy across an illuminant change is to calculate a color constancy index. These indices typically relate the measured shift in the location of the achromatic point to the shift in the chromaticity of a material of uniform spectral reflectance (Brainard 1998). As illustrated in Fig. 4.6, the effect of an illuminant change on cone-coordinates can be well-summarized by multiplicative scaling, and on opponent signals by multiplicative scaling of the $S/L+M$ opponent signal and translational (additive) scaling of the $L/L+M$ opponent signal. We have defined two color constancy indices, one appropriate for dimensions undergoing multiplicative change (Yang & Shevell 2002), and the other for dimensions undergoing additive change. If $b_1$ is the coordinate of Illuminant 1, $b_2$ is the coordinate of Illuminant 2, and $a_1$ and $a_2$ are the respective coordinates of the achromatic settings, then the multiplicative constancy index is defined as $C=(\log(a_1/a_2))/(\log(b_1/b_2))$. The value of $(a_1/a_2)$ reveals the scaling factor used by the multiplicative neural transformation; $b_1/b_2$ quantifies the color conversion imposed by the illuminant change. For perfect constancy $(a_1/a_2) = (b_1/b_2)$ and the index is equal to one. If the co-ordinates of the achromatic settings are not affected by the illuminant, $a_1 = a_2$, and the index is zero. For dimensions undergoing translational scaling, the index is defined as $C = |a_1-a_2|/|b_1-b_2|$. Again, $C = 0$ indicates no constancy, and $C = 1$ indicates perfect constancy. However, since the mapping between chromaticity space and perceptual color space is not known, and is likely to be nonlinear and depend on adaptation state, no constancy index can provide a perceptually accurate measure of how steady a material will appear under an illuminant change.

We derived achromatic points from our data by calculating the point of intersection of the red/green and the blue/yellow classification boundaries. The data showed high levels of constancy, with the averages of the $L$-, $M$-, and $S$-cone constancy indices equal to 0. 87, 0.72, and 0.94, and averages of the $L/(L+M)$ and $S/(L+M)$ constancy indices, equal to 0.87, 0.68, and 0.93 for the three observers.

In the first experiment, the mean chromaticity of the scene could provide a reliable estimate of the cone-coordinates of the illuminant, so good color constancy would be predicted by spatially extended adaptation or alternatively by a high-level mechanism that used the mean to derive an illuminant estimate. In the second experiment, we simulated conditions where the mean chromaticity of the scene does not provide a good estimate of the cone-coordinates of the illuminant. We obtained classification boundaries under four additional conditions. We used sunlight and skylight and red-blue biased, and green-yellow biased sets of reflectances for the background (Fig. 4.11).

Figures 4.12 (left) and (right) show classification boundaries for red-blue and green-yellow biased backgrounds respectively. The red lines represent color boundaries under sunlight and the blue lines represent boundaries under skylight.

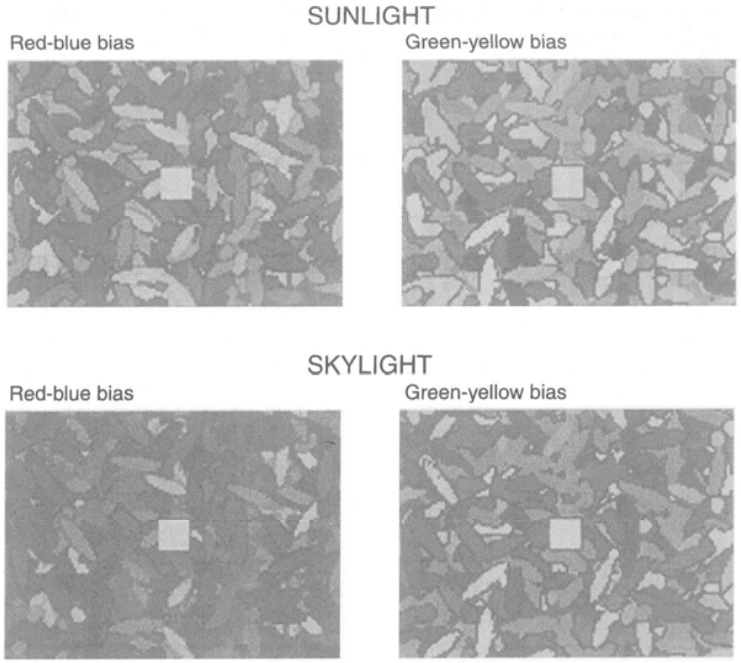


FIG. 4.11 Examples of stimuli used in color appearance measurements with a global illuminant change on chromatically biased backgrounds. The top row shows stimuli rendered under sunlight; the bottom row shows stimuli rendered under skylight. (See also Plate 3 at the centre of this book.)

Again the illuminant has a large effect on the locations of red/green and yellow/blue boundaries in chromaticity space, but the locations of the boundaries in reflectance space are largely unaltered by the illuminant condition. Observers demonstrated high levels of constancy in all conditions. The averages of the $L/(L+M)$ and $S/(L+M)$ constancy indices were 0.87, 0.81, and 0.95 for the three observers.

The results confirm that the color appearance of the test-materials is not set by the mean chromaticity of the global scene. To assess whether performance could be explained by any spatially extended illuminant estimate we performed a critical manipulation. Unknown to the observer, we simulated one illuminant for the test and a different illuminant for the background. Under these conditions, the spatial context provides information only about the background illuminant, so any *global* mechanism would estimate the wrong illuminant for the test, and constancy would be low. In a single trial, the observer has no information about the test-illuminant, since it falls only on a single material and there are no statistical cues to disentangle the material reflectance and the illuminant spectrum. Hence information about the test illuminant is available only by collating information

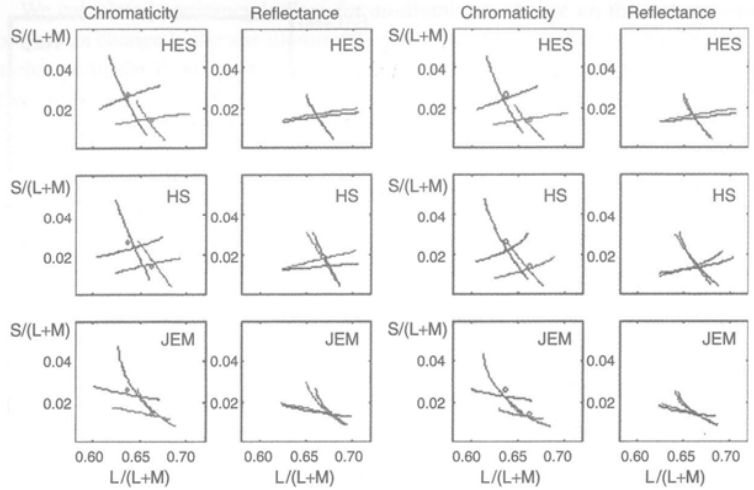


FIG. 4.12 Data for the three observers, with a global illuminant change on (Left) red-blue biased backgrounds, (Right) green-yellow biased backgrounds. Panels on the left show traces of classification boundaries in chromaticity space, obtained under sunlight (red lines) or skylight (blue lines). Open-circles show the corresponding illuminant chromaticities. Panels on the right show the same boundaries represented in reflectance space (i.e. as if materials were rendered under an equal energy illuminant). (See also Plate 4 at the centre of this book.)

over successive trials. We asked whether the classification of test-materials in the inconsistent illuminant conditions follows that predicted by the background illuminant, or that predicted by the test illuminant. Again, stimulus displays comprised a central square test-patch within a variegated background of elliptical patches. We used the balanced set of background materials, but rather than using a global illuminant for the whole scene, we either rendered the test-material under sunlight and the background materials under skylight, or the test-material under skylight and the background materials under sunlight (Fig. 4.13 (left)).

The dotted lines in Fig. 4.13 (right) show classification boundaries re-plotted from the first experiment. They are color-coded according to the global illumination used: red for sunlight and blue for skylight. The solid lines show classification boundaries for the inconsistent illumination conditions, and are color-coded according to the illuminant falling on the test-patch. So, red lines show performance with sunlight on the test and skylight on the background, and blue lines show performance with skylight on the test and sunlight on the background. Performance in the inconsistent illumination conditions is more closely predicted by the illuminant falling on the test-patch than by the illuminant falling on the background. For observer HS, the blue-yellow boundary was not well-constrained by our data for the condition with sunlight on the test and skylight on the background.

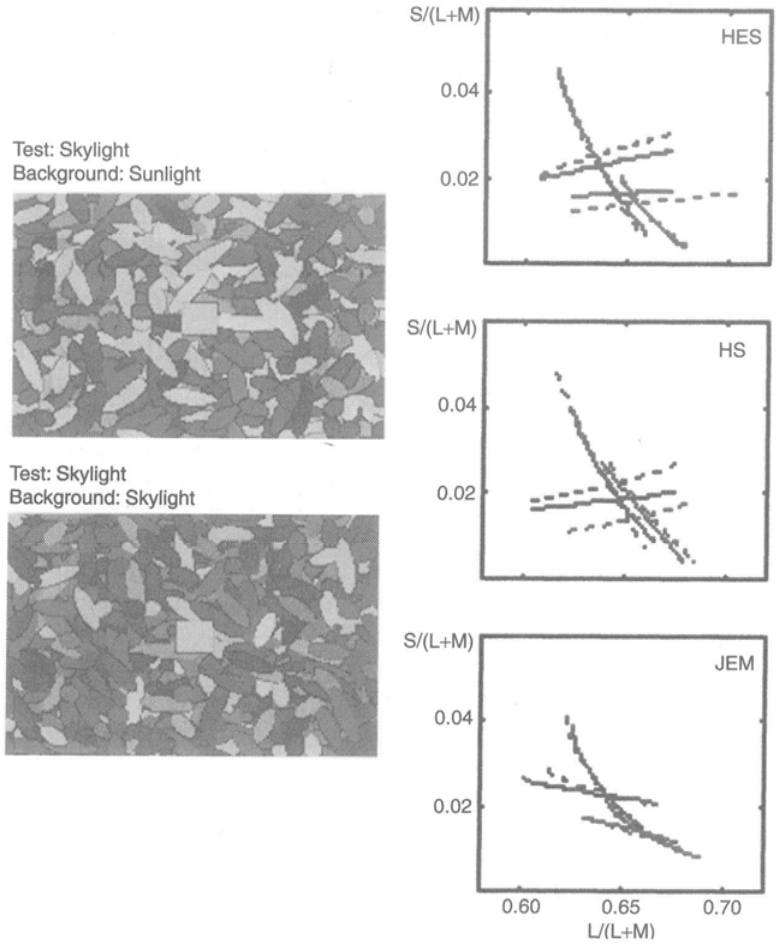


FIG. 4.13 (Left) Examples of stimuli used in color appearance measurements with conflicting illuminants on test and background reflectances. (Right) Data for the three observers. Solid red lines indicate classification boundaries obtained with sunlight illumination on the test, and skylight on the background. Solid blue lines indicate classification boundaries obtained with skylight on the test, and sunlight on the background. Dotted red and blue lines show boundaries obtained with a global illuminant of sunlight or skylight respectively, and are thus color-coded to predict boundary locations based on the test illuminant. Discriminant functions for Observer HS, with sunlight on the test and skylight on the background, were not well-constrained. (See also Plate 5 at the centre of this book.)

We calculated constancy indices for an illuminant change on the test-material only, i.e. a change in the test-illuminant coordinates from $b_1$ to $b_2$. In this analysis, a change in the illuminant on the test is not accompanied by a corresponding change in the illuminant on the background, so the spatial context provides no cues to the illuminant change, signalling instead either steady sunlight or skylight. So, if performance were determined by the spatial context, the achromatic coordinates ($a_1$ and $a_2$) should be identical, and we should measure constancy indices equal to zero. If however performance were determined by the test illuminant, constancy indices should approach one (or rather the value obtained in the first experiment for a global illuminant change). The averages of the $L/(L+M)$ and $S/(L+M)$ constancy indices were 0.70, 0.45, and 0.82 for the three observers. Constancy indices are in all cases slightly lower than those obtained in the first experiment, but constancy is far from abolished. Observers' performances cannot be explained by any spatially extended process, since the spatial context provided cues to the wrong illuminant. The type of neural mechanism that could perform this temporal collation process could be peripheral or central. A process of spatially localized adaptation, with long time-constants of the order of a few seconds, would converge on the mean chromaticity of the test-materials. Since the mean chromaticity of the test materials was balanced, this would be sufficient to support reasonable constancy.

Early adaptation is not the only neural transformation that could use estimated illuminant cone-coordinates. Later perceptual mechanisms could use these estimates to adjust for color conversions (Adelson & Pentland 1996), without losing information about the illuminant color (Zaidi 1998). For example, Khang & Zaidi (2002) showed that observers were able to identify like versus unlike objects across illuminants, based on perceived similarities between color-shifts of backgrounds and color-shifts of tests. Such non-adaptation mechanisms are particularly salient when the geometrical properties of the scene promote color scission, i.e. separation of the colors of the scene into material colors and the colors of illuminants or transparencies (Hagedorn & D'Zmura 2000).

A different class of transformation mechanism involves the concept of "level of reference" or "anchoring" (Rogers 1941; Helson 1947). Thomas & Jones (1962) showed that matches to a reference color were biased by the distribution of possible matching colors. In its extreme form, if perceived colors in a scene were determined entirely by rank-orders of cone-coordinates, good color constancy would be the result because, as shown in Fig. 4.6, color conversions do not disturb rank-orders of cone-coordinates. This mechanism would not need an estimate for the illuminant but would, like adaptation to the mean, lead to inconstancy if the set of available materials changed.

Our final experiment was designed to determine whether the neural processes that collate information about a temporally extended sample of illuminated spectral reflectances are automatic, or whether they are based on perceptual processes that are selective for information about the test stimuli. We used conflicting illuminants for test and background but now reduced the

amount of time observers were exposed to the test-patches to a fraction of the duration of exposure to materials illuminated by the background illuminant. As for all experiments reported here, trial duration was fixed at 1500 ms. But now the test-materials were presented only for 200 ms, after which the display reverted to the background pattern. An automatic adaptation process collates information indiscriminately from test and background. If color constancy is achieved under the test illuminant it must be based on a selective mechanism that collates only the test samples.

The three observers were differently influenced by the reduction in exposure to the test illuminant. For HES, the boundaries obtained with skylight on the test and sunlight on the background were now well-predicted by performance with global sunlight illumination. The red-green boundary obtained with sunlight on the test and skylight on the background was also clearly consistent with the background illuminant, likewise for HS. However, for HS and JEM, the boundaries obtained with skylight on the test and sunlight on the background were well-predicted by the test illuminant. Similarly, the constancy indices indicated that constancy was practically abolished for HES, but remained reasonably high in at least one condition for HS and JEM.

The mixed performance in the final experiment cannot be completely explained by an automatic neural process that acts upon incoming chromatic signals to discount the illuminant. However, in some conditions, observers' judgments were consistent with the hypothesis that the test-materials are illuminated by a different illuminant from the background. In a single trial there is no information about the test illuminant (since this falls only on a single material) so information about the test illuminant can only be obtained by collating information from successive trials. To collate the properties of the test illuminant separately from the properties of the background illuminant requires a process that tracks the chromatic statistics of the task-relevant test-squares. Such a process could be a mechanism of adaptation gated by attention, or it may be a perceptual "level of reference" or "anchoring" (Rogers 1941; Helson 1947) mechanism that segregates test and background presentations. Several cues distinguish test from background. The most obvious is that the test-squares require a judgment while the background ellipses do not. A more subtle cue is highlighted in Forsyth's constancy algorithm (Forsyth 1990). Since the illuminant limits the gamut of spectra reaching the eye, it is possible that (due to the conflicting illuminant) the colors of the test were very unlikely under the background illuminant, and this might provide a cue for the visual system to estimate the illuminant separately for the test-patches.

The majority of experiments on color constancy have focused on the spatial information available in a scene. The primary message from the Smithson and Zaidi (2004) study is that the stability of color appearance is determined mainly by local mechanisms that collate information over time. The color-appearance judgments obtained with conflicting illuminants could be predicted by mechanisms that are either spatially local in extent or that segregate the test from the background. Therefore it is uncertain whether temporal context acts centrally to modify the observer's "adaptation-level" (Helson 1947, 1964), or whether the information reaching the decision-stage is modified automatically by peripheral mechanisms. In certain conditions and for certain observers, the drastic decrease in constancy as a result of reducing exposure to the test is consistent with an adaptation mechanism with a long time constant. However, in other conditions there is little decrease in constancy, indicating the use of a central value that stores contextual information about the stimuli requiring judgment.

## 4.7 Summary

This paper starts with an example involving lightness identification of 3-D objects across illuminants differing in mean radiance. We show that observers use brightness similarity between materials to perform the lightness identification task, and adaptation serves to make like materials more similar in brightness across illuminants than if luminance is used to judge similarity. The effect of a change in illuminant radiance is to multiply the luminance of all objects in a scene with the same constant, since the luminance of each object is the product of its reflectance and the illuminant radiance. On the other hand, the effect of a change in the spectrum of the illuminant is different for different materials in the field of view since it depends on the spectral reflectance of each material. However, if the effect is calculated in terms of cone-coordinates, then the situation is considerably simplified. Within each cone class, the effect is decently approximated by multiplication by the same constant for all materials. This suggests that if the cone-coordinates of the illuminant can be estimated, then a neural process could invert the effect. We show that when observers are asked to estimate the color of a spotlight, they use a scene statistic that is approximately equal to the mean cone-coordinates of the brightest objects in the scene. Global adaptation to the scene, however, does not use similar statistics, and has limited effectiveness as a color constancy mechanism. On the other hand, spatially local adaptation does play a large role in color constancy. We show that observers can invert the effect of illuminant spectrum changes by collating local information over time. This information seems to be used both in adaptation processes, and in setting levels of reference.

### Acknowledgments

The research described in this paper was done in collaboration with Arthur Shapiro, Ben Sachtler, Bill Yoshimi, Branka Spehar, Jeremy DeBonet, Byung-Geun Khang, Hannah Smithson, and Rocco Robillotto. This work was supported by NEI grant EY07556.

## References


Adelson, E.H., & Pentland, A.P. (1996). The perception of shading and reflectance. In D. C. Knill, & W. Richards (Eds.), *Perception as Bayesian Inference* (pp. 409–23). Cambridge: Cambridge University Press.

Baylor, D.A., Nunn, B.J., & Schnapf, J.L. (1987). Spectral sensitivity of cones of the monkey Macaca fascicularis. *Journal of Physiology*, *390*, 145–60.

Brainard, D.H. (1998). Color constancy in the nearly natural image. 2. Achromatic loci. *Journal of the Optical Society of America A*, *15*(2), 307–25.

Brainard, D.H., & Wandell, B.A. (1992). Asymmetric color matching: how color appearance depends on the illuminant. *Journal of the Optical Society of America A*, *9*(9), 1433–8.

Brown, R.O. (1994). The world is not gray. *Investigative Ophthalmology & Visual Science*, *35*(4), 2165.

Buchsbaum, G. (1980). A spatial processor model for object color perception. *Journal of the Franklin Institute*, *310*, 1–26.

Chevreul, M.E. (1839). *De la loi du contraste simultane des couleurs*. Paris: Pitois-Levreault.

Chichilnisky, E.J., & Wandell, B.A. (1999). Trichromatic opponent color classification. *Vision Research*, *39*(20), 3444–58.

Chittka, L., Shmida, A., Troje, N., & Menzel, R. (1994). Ultraviolet as a component of flower reflections, and the color perception of Hymenoptera. *Vision Research*, *34*(11), 1489–1508.

Craik, K.J.W. (1938). The effect of adaptation on differential brightness discrimination. *Journal of Physiology*, *92*, 406–21.

Dannemiller, J.L. (1993). Rank orderings of photoreceptor photon catches from natural objects are nearly illuminant-invariant. *Vision Research*, *33*, 131–40.

Derrington, A.M., Krauskopf, J., & Lennie, P. (1984). Chromatic mechanisms in lateral geniculate nucleus of macaque. *Journal of Physiology*, *357*, 241–65.

D'Zmura, M., & Lennie, P. (1986). Mechanisms of color constancy. *Journal of the Optical Society of America A*, *3*(10), 1662–72.

Evans, R.M. (1974). *The Perception of Color*. New York: Wiley & Sons.

Fairchild, M.D., & Lennie, P. (1992). Chromatic adaptation to natural and incandescent illuminants. *Vision Research*, *32*(11), 2077–85.

Forsyth, D. (1990). A novel algorithm for color constancy. *International Journal of Computer Vision*, *30*, 5–36.

Foster, D.H. (2003). Does color constancy exist? *Trends in Cognitive Sciences*, *7*(10), 439–43.

Foster, D.H., & Nascimento, S.M. (1994). Relational color constancy from invariant cone-excitation ratios. *Proceedings of the Royal Society of London B Biological Sciences*, *257*(1349), 115–21.

Golz, J., & MacLeod, D.I. (2002). Influence of scene statistics on color constancy. *Nature*, *415*(6872), 637–40.

Hagedorn, J., & D'Zmura, M. (2000). Color appearance of surfaces viewed through fog. *Perception*, *29*(10), 1169–84.

Hayhoe, M.M., Benimoff, N.I., & Hood, D.C. (1987). The time-course of multiplicative and subtractive adaptation process. *Vision Research*, *27*(11), 1981–96.

He, S., & MacLeod, D.I. (1998). Local nonlinearity in S-cones and their estimated light-collecting apertures. *Vision Research*, *38*(7), 1001–6.





Helmholtz, H.v. (1962). *Physiological Optics*. Trans. Vol. 3, J.P.C. Southhall. New York: Dover.

Helson, H. (1938). Fundamental problems in color vision. I. The principle governing changes in hue, saturation, and lightness of non-selective samples in chromatic illumination. *Journal of Experimental Psychology*, *23*, 439–76.

Helson, H. (1947). Adaptation-level as frame of reference for prediction of psychophysical data. *Journal of the Optical Society of America*, *60*, 1–29.

Helson, H. (1964). *Adaptation-level Theory; An Experimental and Systematic Approach to Behavior*. New York: Harper & Row.

Helson, H., Judd, D.B., & Warren, M.H. (1952). Object-color changes from daylight to incandescent filament illumination. *Illuminating Engineering*, *47*, 221–3.

Hering, E. (1964). *Outlines of a Theory of the Light Sense*. Trans. L.M. Hurvich, & D. Jameson. Cambridge, MA: Harvard University Press.

Hiltunen, J. (1996). *Munsell Color Matts (Spectrophotometer Measurements by Hiltunen)*. Retrieved September 10, 1999, from http://www.it.lut.fi/ip/research/color/database/download.html#munsell_spec_matt

Ives, H.E. (1912). The relation between the color of the illuminant and the color of the illuminated object. *Transactions of the Illuminating Engineering Society*, *7*, 62–72.

Khang, B.G., & Zaidi, Q. (2002). Cues and strategies for color constancy: perceptual scission, image junctions and transformational color matching. *Vision Research*, *42*(2), 211–26.

Khang, B.G., & Zaidi, Q. (2004). Illuminant color perception of spectrally filtered spotlights. *Journal of Vision*, *4*, 680–92.

Kingdom, F. (2003). Color brings relief to human vision. *Nature Neuroscience*, *6*(6), 641–4.

Koenderink, J.J., & van Doorn, A.J. (1996). Illuminance texture due to surface mesostructure. *Journal of the Optical Society of America A*, *13*, 452–63.

Kraft, J.M., & Brainard, D.H. (1999). Mechanisms of color constancy under nearly natural viewing. *Proceedings of the National Academy of Sciences USA*, *96*(1), 307–12.

Land, E.H. (1983). Recent advances in retinex theory and some implications for cortical computations: color vision and the natural image. *Proceedings of the National Academy of Sciences USA*, *80*(16), 5163–69.

Land, E.H., & Mc Cann, J.J. (1971). Lightness and retinex theory. *Journal of the Optical Society of America*, *61*, 1–11.

Lee, H.C. (1986). Method for computing the scene-illuminant chromaticity from specular highlights. *Journal of the Optical Society of America A*, *3*(10), 1694–9.

Lehmann, T.M., & Palm, C. (2001). Color line search for illuminant estimation in real-world scenes. *Journal of the Optical Society of America A*, *18*(11), 2679–91.

MacLeod, D.I., & Boynton, R.M. (1979). Chromaticity diagram showing cone excitation by stimuli of equal luminance. *Journal of the Optical Society of America*, *69*(8), 1183–6.

MacLeod, D.I., & He, S. (1993). Visible flicker from invisible patterns. *Nature*, *361*(6409), 256–8.

MacLeod, D.I., Williams, D.R., & Makous, W. (1992). A visual nonlinearity fed by single cones. *Vision Research*, *32*(2), 347–63.

Marshall, N.J. (2000). Communication and camouflage with the same 'bright' colors in reef fishes. *Philosophical Transactions of the Royal Society of London B Biological Sciences*, *355*(1401), 1243–8.

Nascimento, S.M., Ferreira, F.P., & Foster, D.H. (2002). Statistics of spatial cone-excitation ratios in natural scenes. *Journal of the Optical Society of America A*, *19*(8), 1484–90.

Nascimento, S.M., & Foster, D.H. (1997). Detecting natural changes of cone-excitation ratios in simple and complex colored images. *Proceedings of the Royal Society of London B Biological Sciences*, *264*(1386), 1395–1402.

Oren, M., & Nayar, S.K. (1995). Generalizations of the Lambertian model and implications for machine vision. *International Journal of Computer Vision*, *14*, 227–51.

Robilotto, R., and Zaidi, Q. (2004). Limits of lightness identification for real objects under natural viewing conditions. *Journal of Vision*, *4*, 779–97.

Rogers, S. (1941). The anchoring of absolute judgments. *Archives of Psychology Columbia University*, *261*, 42.

Sachtler, W.L., & Zaidi, Q. (1992). Chromatic and luminance signals in visual memory. *Journal of the Optical Society of America A*, *9*, 877–94.

Shapiro, A., Beere, J., & Zaidi, Q. (2001). Stages of temporal adaptation in the RG color system. *Color Research and Application*, *26*, S43–S47.

Shapiro, A., Beere, J., & Zaidi, Q. (2003). Time course of adaptation stages in the S cone color system. *Vision Research*, *43*, 1135–47.

Sinha, P., & Adelson, E.H. (1993). Recovering reflectance and illumination in a world of painted polyhedra. *Proceedings of the Fourth International Conference on Computer Vision* (pp. 156–63). Los Alamitos, CA: IEEE Computer Society Press.

Smith, V.C., & Pokorny, J. (1975). Spectral sensitivity of the foveal cone photopigments between 400 and 500 nm. *Vision Research*, *15*(2), 161–71.

Smithson, H., & Zaidi, Q. (2004). Color constancy in context: roles of local adaptation and reference levels. *Journal of Vision*, *4*, 693–710.

Taylor, A.H., & Kerr, G.P. (1941). The distribution of energy in the visible spectrum of daylight. *Journal of the Optical Society of America*, *31*(1), 3–8.

Thomas, D.R., & Jones, C.G. (1962). Stimulus generalization as a function of the frame of reference. *Journal of Experimental Psychology*, *64*(1), 77–80.

Tominaga, S., Ebisui, S., & Wandell, B.A. (2001). Scene illuminant classification: brighter is better. *Journal of the Optical Society of America A*, *18*(1), 55–64.

Vimal, R.L., Pokorny, J., & Smith, V.C. (1987). Appearance of steadily viewed lights. *Vision Research*, *27*(8), 1309–18.

von Kries, J. (1878). Physiology of visual sensations. In D.L. MacAdam (ed.), *Sources of Color Science* (pp. 101–8). Cambridge, MA: MIT Press.

von Kries, J. (1905). Die Gesichtsempfindungen. In W. Nagel (ed.), *Handbuch der Physiologie des Menschen* (Vol. 3) Physiologie der Sinne. Braunschweig: Vieweg und Sohn.

Vrhel, M., Gershon, R., & Iwan, L.S. (1994). Measurement and analysis of object reflectance spectra. *Color Research and Application*, *19*, 4–9.

Webster, M.A. (1996). Human color perception and its adaptation. *Network: Computation in Neural Systems*, *7*(4), 587–634.

Webster, M.A., Malkoc, G., Bilson, A.C., & Webster, S.M. (2002). Color contrast and contextual influences on color appearance. *Journal of Vision*, *2*(6), 505–19.

Webster, M.A., & Mollon, J.D. (1997). Adaptation and the color statistics of natural images. *Vision Research*, *37*(23), 3283–98.

Yang, J.N., & Shevell, S.K. (2002). Stereo disparity improves color constancy. *Vision Research*, *42*(16), 1979–89.

Zaidi, Q. (1998). Identification of illuminant and object colors: heuristic-based algorithms. *Journal of the Optical Society of America A*, *15*(7), 1767–76.

Zaidi, Q. (1999). Color and brightness induction: From Mach bands to 3-D configurations. In K. Gegenfurtner, & L. Sharpe (ed.), *Color Vision: From Genes to Perception*. Cambridge: Cambridge University Press.

Zaidi, Q. (2001). Color constancy in a rough world. *Color Research and Application*, *26*(S1), S192–S200.

Zaidi, Q., & Shapiro, A., (1993). Adaptive orthogonalization of opponent-color signals. *Biological Cybernetics*, *69*, 415–28.

Zaidi, Q., Shapiro, A., & Hood, D. (1992). The effect of adaptation on the differential sensitivity of the S-cone color system. *Vision Research*, *32*, 1297–1318.

Zaidi, Q., Spehar, B., & DeBonet, J. (1997). Color constancy in variegated scenes: role of low-level mechanisms in discounting illumination changes. *Journal of the Optical Society of America A*, *14*(10), 2608–21.

Zaidi, Q., Spehar, B., and DeBonet, J. (1998). Adaptation to textured chromatic fields. *Journal of the Optical Society of America A*, *15*, 23–32.

Zaidi, Q., Yoshimi, B., Flanigan, N., & Canova, A. (1992). Lateral interactions within color mechanisms in simultaneous induced contrast. *Vision Research*, *32*(9), 1695–1707.

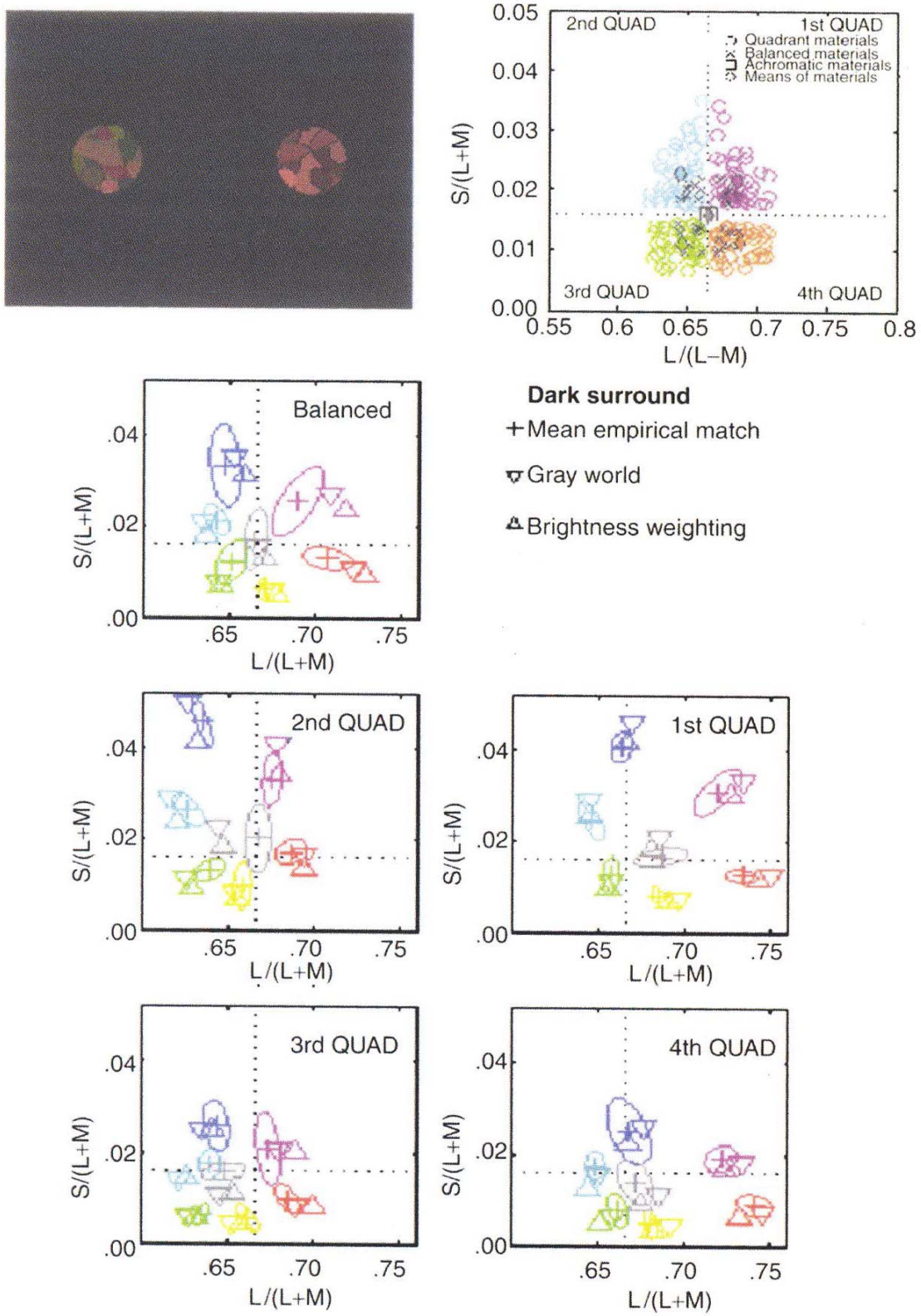


PLATE 1 (Top left) Red spotlight cast on green-yellow materials on the left and the same red spotlight on gray materials on the right. Observers were asked to estimate the color of the spotlight moving on chromatic materials and to match it by adjusting the color of the spotlight moving on gray materials. (Top right) MacLeod–Boynton chromaticities (under equal energy light) of the 240 materials used, which consisted of 6 sets of 40 materials, 4 sets of chromatic materials from each quadrant, one set of balanced chromatic materials, one set of achromatic materials. Colored diamonds indicate mean of each quadrant's materials, while the square and the gray diamond at the intersection of the horizontal and vertical dotted lines represent both the achromatic materials and the mean of the balanced chromatic materials. (Bottom) Mean chromaticities of the match spotlights (+), and predictions from a gray-world model (△) and a model that gives greater weight to the brighter materials (▽). The results are color-coded to correspond roughly to the

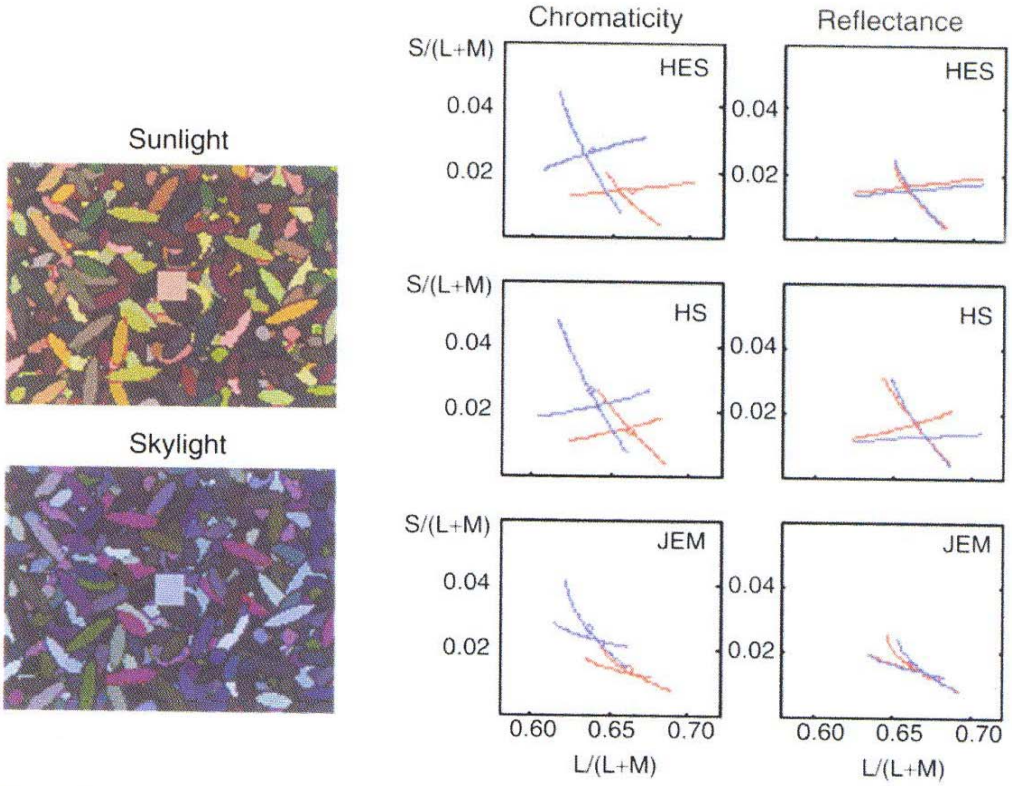


PLATE 2 (Left) Examples of stimuli used in color appearance measurements with a global illuminant change on chromatically balanced backgrounds. On each trial, a square test patch was presented on a variegated background of randomly oriented elliptical patches, under skylight or sunlight. (Center) Data for three observers. Panels show traces of classification boundaries in chromaticity space. Red lines show boundaries obtained under sunlight; blue lines show boundaries obtained under skylight. Red and blue open-circles show the corresponding illuminant chromaticities. (Right) Panels show the same boundaries represented in reflectance space (i.e. as if materials were rendered under an equal energy illuminant). (See also Chapter 4, Fig. 4.10.)

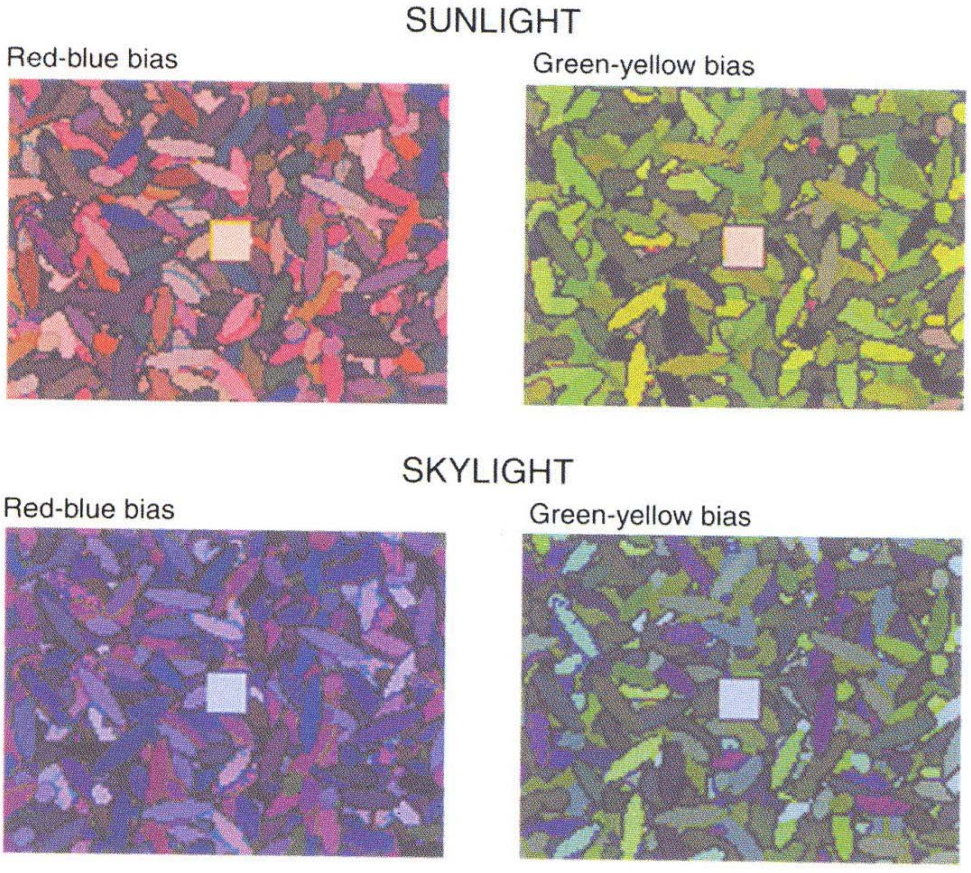


PLATE 3. Examples of stimuli used in color appearance

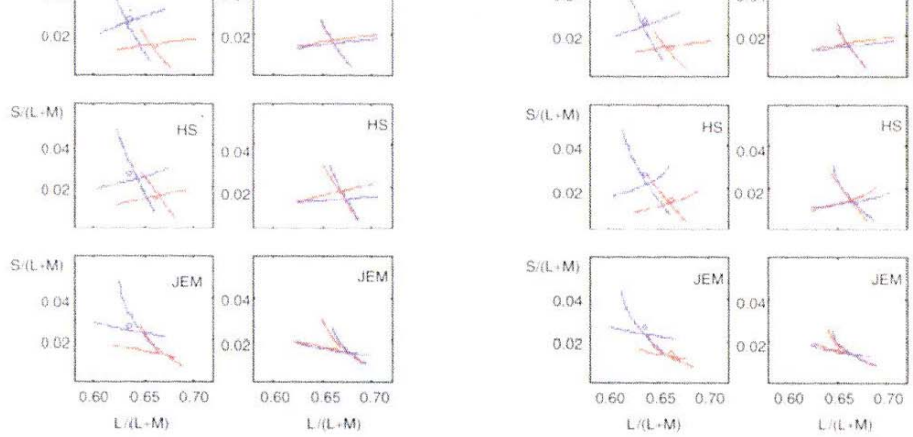


PLATE 4 Data for the three observers, with a global illuminant change on (Left) red-blue biased backrounds, (Right) green-yellow biased backrounds. Panels on the left show traces of classification boundaries in chromaticity space, obtained under sunlight (red lines) or sky light (blue lines). Open-circles show the corresponding illuminant chromaticities. Panels on the right show the same boundaries represented in reflectance space (i.e. as if materials were rendered under an equal energy illuminant). (See also Chapter 4, Fig. 4.12.)

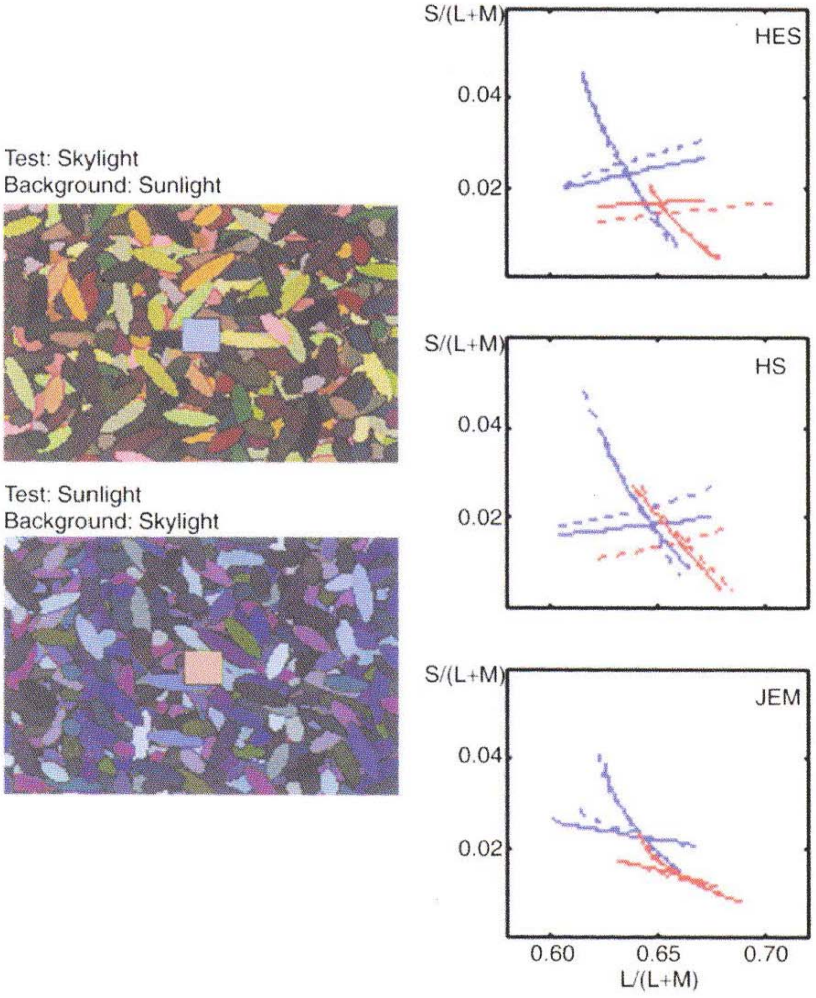


PLATE 5 (Left) Examples of stimuli used in color appearance measurements with conflicting illuminants on test and background reflectances. (Right) Data for the three observers. Solid red lines indicate classification boundaries obtained with sunlight illumination on the test, and skylight on the background. Solid blue lines indicate classification boundaries obtained with skylight on the test, and sunlight on the background. Dotted red and blue lines show boundaries obtained with a global illuminant of sunlight or skylight respectively, and are thus color-coded to predict boundary locations based on the test illuminant. Discriminant functions for

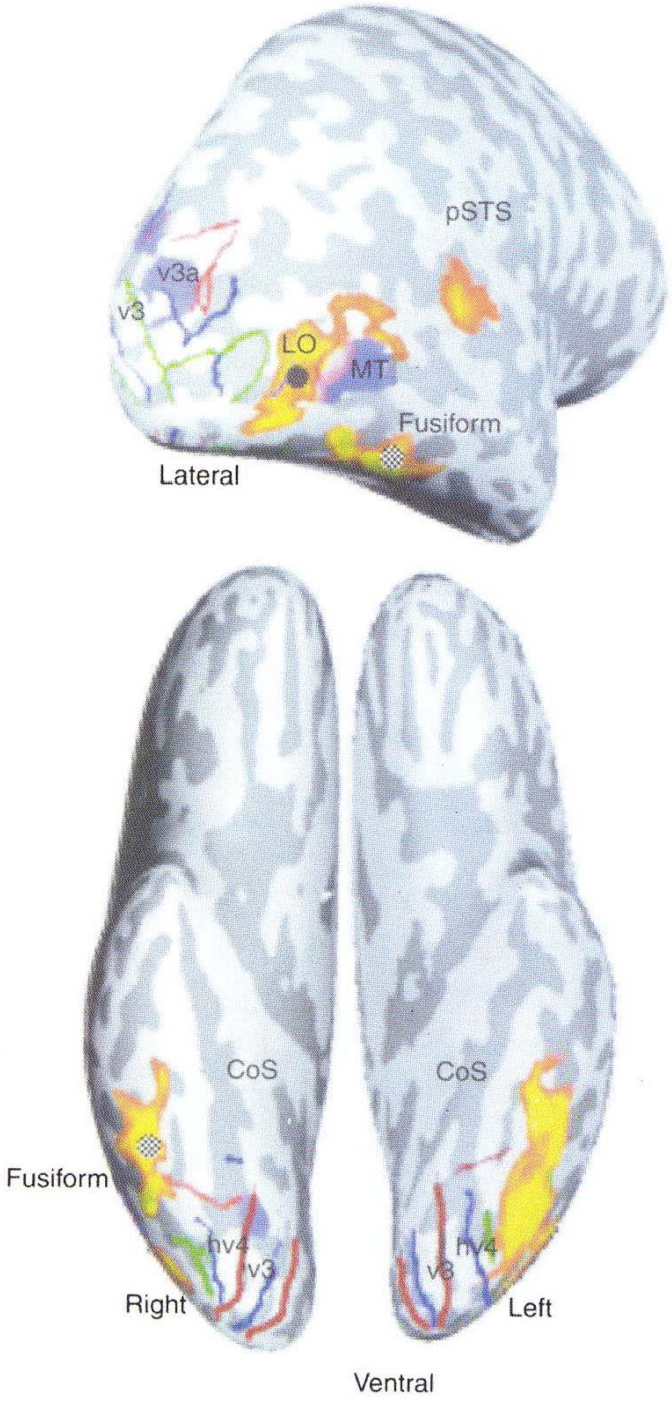


PLATE 6 Regions that activate to faces more strongly than novel objects, houses, cars, and scenes with $p < 10^{-4}$ at the voxel level. Lines indicate visual meridians: blue: horizontal visual meridian; red: upper visual meridian; green: lower visual meridian. Location of MT is indicated in blue. Three main regions show higher activation for faces compared to controls: a region in the fusiform gyrus, a region in LO, and a region in the posterior STS. (See also Chapter 6, Fig. 6.5.)